

Deep Plug-and-Play Prior for Parallel MRI Reconstruction

Ali Pour Yazdanpanah^{1,2} Onur Afacan^{1,2} Simon K. Warfield^{1,2}

¹Harvard Medical School

²Boston Children’s Hospital

{ali.pouryazdanpanahkermani, onur.afacan, simon.warfield}@childrens.harvard.edu

Abstract

Fast data acquisition in Magnetic Resonance Imaging (MRI) is vastly in demand and scan time directly depends on the number of acquired k -space samples. Conventional MRI reconstruction methods for fast MRI acquisition mostly relied on different regularizers which represent analytical models of sparsity. However, recent data-driven methods based on deep learning has resulted in promising improvements in image reconstruction algorithms. In this paper, we propose a deep plug-and-play prior framework for parallel MRI reconstruction problems which utilize a deep neural network (DNN) as an advanced denoiser within an iterative method. This, in turn, enables rapid acquisition of MR images with improved image quality. The proposed method was compared with the reconstructions using the clinical gold standard GRAPPA method. Our results with under-sampled data demonstrate that our method can deliver considerably higher quality images at high acceleration factors in comparison to clinical gold standard method for MRI reconstructions. Our proposed reconstruction enables an increase in acceleration factor, and a reduction in acquisition time while maintaining high image quality.

1. Introduction

Parallel imaging (PI) techniques have become popular strategies for reducing scan time, such as by undersampling phase encodes in different MRI sequences, and for mitigating geometric distortion, such as in EPI sequences. PI uses spatially varying coil sensitivity profiles from an array of receiver coils, to reconstruct images despite undersampling of data. Two primary PI reconstruction algorithms are the image domain method of sensitivity encoding (SENSE) [22] and the frequency domain method of generalized autocalibrating partially parallel acquisitions (GRAPPA) [6]. SENSE reconstruction is achieved by solving a linear system of equations that uses the coil sensitivity profiles. Efficient reconstruction methods have been introduced based on the SENSE framework for both Cartesian

[22], and non-Cartesian trajectories [21]. SENSE-based methods, that explicitly require the coil array sensitivity maps to be known, include parallel MRI with adaptive radius in k -space (PARS) [34], parallel imaging reconstruction for arbitrary trajectories using k -space sparse matrices (kSPA) [18], and sensitivity profiles from an array of coils for encoding and reconstruction in parallel (SPACE-RIP) [16]. The PARS approach performs point-by-point reconstruction by creating and inverting small localized encoding matrices (lies within a small radius in k -space) instead of inverting the complete encoding matrix at once. The kSPA approach performs the reconstruction as a system of sparse linear equations in k -space which is achieved by computing a sparse approximate inverse matrix. The SPACE-RIP approach positions RF receiver coils around the object of interest which make it possible to image different plane within the volume of interest and also enabling variable density sampling in k -space.

GRAPPA reconstruction is an autocalibrating method based on local k -space kernels, which utilize the learned correlation between multiple channels in local areas and fill missing k -space values by a linear combination of the acquired local data from multiple coils. Partially parallel imaging with localized sensitivities (PILS) [7], simultaneous acquisition of spatial harmonics (SMASH) [26], AUTO-SMASH [13], and VD-AUTO-SMASH [12], are other examples of autocalibrating methods which utilize k -space kernels. The PILS approach needs specific coil arrangement in order to reconstruct the full field of view. The receiver coils in PILS approach located linearly in the direction of phase encoding with localized sensitivities over different regions in the full field of view. The SMASH approach, generates missing data directly by a weighted linear combination of the estimated sensitivity maps. The weights in SMASH are estimated by fitting the maps to spatial harmonic of specific order. The AUTO-SMASH approach exploits a few numbers of autocalibration signal (ACS) lines to estimate the sensitivities. Variable-density AUTO-SMASH (VD-AUTO-SMASH) uses multiple ACS lines from the k -space center to improve the reconstruction

of the AUTO-SMASH approach. GRAPPA approach can be considered as a generalized version of the VD-AUTO-SMASH approach. GRAPPA techniques have been extended to non-Cartesian k -space trajectories by the methods such as [25, 11]. Iterative self-consistent parallel imaging reconstruction (SPIRIT) [20] method is also based on GRAPPA framework but formulated as an inverse problem which can reconstruct data from arbitrary k -space trajectories. The extended version of SPIRIT method was introduced in [29] (ESPIRIT) which considered to reconstruct missing data by restricting the solution to a subspace and estimate the sensitivity maps from autocalibration lines in k -space using eigenvalue decomposition of k -space filtered calibrated kernels in image space.

It is also possible to reduce the aliasing artifact through techniques such as 2D CAIPIRINHA [4], and Wave-CAIPI [2], both of which modify the data acquisition in order to reduce the concentration of aliasing artifacts on certain regions, leading to a reduced geometry factor penalty, and a more robust reconstruction.

A popular approach to reduce or mitigate the presence of reconstruction artifacts has been regularized reconstruction or compressed sensing (CS) method. Methods based on SENSE are particularly reformulated to include regularization [23], and rapid and accurate reconstructions are possible. Popular regularization constraints include gradient norm, total variation, and l_1 -norm of transform domain coefficients to promote edge preservation and sparsity. CS methods seek to exploit intrinsic image properties of sparsity in a transform domain and have allowed for highly accelerated imaging in different settings. These techniques allow for images to be reconstructed with the similar linear algebra equation that express both data similarity term and sparsity penalty term. These have allowed to increase data acquisition speed while generating better reconstructions [23, 19, 17, 1, 8, 32, 33, 9]. Due to nondifferentiability of some regularizers, proximal methods like alternating direction method of multipliers (ADMM) [3] has been proposed. Proximal methods uses proximal operator to avoid the regularizer differentiation. The plug-and-play prior framework [30] presented with an idea to utilize the denoiser without any regularization objective as proximal operator in an iterative method for image recovery. The method has been used in different imaging inverse problem applications [27, 5, 14, 28]. In [27], authors used the plug-and-play framework for bright field electron tomography. In [5], plug-and-play alternating direction method of multipliers has been used for image restoration applications. In [14], the authors developed the fast-iterative shrinkage/thresholding algorithm (FISTA) variant of plug-and-play prior for model-based nonlinear inverse scattering and proved that the framework is applicable beyond linear inverse problems. In [28], the authors

introduced a scalable version of plug-and-play framework based on iterative shrinkage/thresholding algorithm (ISTA) which utilized a subset of measurement at every iteration in order to parallelize the algorithm. In all the mentioned papers, a fixed denoiser has been used as the proximal operator which its accuracy can't be ideal in different scenarios for different applications. However, in this paper we present a learning-based plug-and-play prior framework for parallel MRI reconstruction which extends the framework to its data-adaptive variant and provides an end-to-end reconstruction scheme. We evaluate the reconstruction performance of our method to clinically-used GRAPPA method. GRAPPA reconstruction method is being considered as the clinical gold standard and the most trusted method by radiologist for MRI reconstruction.

2. Methods

The complete MR imaging model given by

$$d_l(k_m) = \int S_l(\rho)x(\rho)e^{-i2\pi k_m \rho} d\rho + n_l(k_m). \quad (1)$$

where $d_l(k_m)$ is the data-samples measurements from l_{th} coil at the m_{th} k -space location k_m . $n_l(k_m)$ is the noise measured from l_{th} coil at the m_{th} k -space location. $x(\rho)$ is the samples of unknown MR image to be recovered. S_l is the sensitivity map of the l_{th} coil. The following MR imaging model is the discretized version of Equation (1):

$$d = Ex + n. \quad (2)$$

where x is the samples of unknown MR image, $E = PFS$ is an encoding matrix, F is a Fourier matrix. P is a mask representing k -space undersampling pattern and $S = [S_1 \dots S_L]$, S_l is a matrix representing the sensitivity map of the l_{th} coil, $1 \leq l \leq L$, and L is the total number of coils.

Assuming without loss of generality that the inter-coil noise covariance has been whitened, the imaging model can be solved and reach the optimal maximum likelihood estimate for x when E has full column rank. This can be done by solving the following least squares problem

$$\hat{x} = \underset{x}{\operatorname{argmin}} \frac{1}{2} \|d - Ex\|_2^2 \quad (3)$$

which results in

$$\hat{x} = (E^H E)^{-1} E^H d \quad (4)$$

In a case of undersampled k -space data, Equation (4) yields artifacts depending on the sampling pattern. If we consider Cartesian-type sampled k -space, then we create aliasing artifacts in the coil images.

Equation (3) can be poorly-conditioned in a case of high acceleration factor, and therefore, a regularization term can be incorporated additionally in the least-square approach. Assuming that the interchannel noise covariance has been whitened, the reconstruction relies on the regularized least-square approach:

$$\hat{x} = \underset{x}{\operatorname{argmin}} \frac{1}{2} \|d - \text{PFS}x\|_2^2 + \beta R(x) \quad (5)$$

where R is a regularization functional that promotes sparsity in the solution and $\beta > 0$ controls the intensity of the regularization.

Our iterative deep plug-and-play prior framework based on ADMM for solving the Equation (5) is provided in Algorithm 1.

Algorithm 1 Deep Plug-and-Play Prior

Input: $x^0, d, S, u^0 = 0, \lambda > 0$

- 1: **for** $i = 1, 2, \dots, N$ **do**
 - 2: $a^i \leftarrow \operatorname{prox}(d, S, x^{i-1} - u^{i-1}; \lambda)$
 - 3: $\tilde{x}^i \leftarrow \text{DNN}(a^i + u^{i-1})$
 - 4: $u^i \leftarrow u^{i-1} + (a^i - \tilde{x}^i)$
 - 5: **end for**
-

$x^0 = E^H d$ is used as an initialization to the algorithm. For least-square cases, we have

$$\operatorname{prox}(d, S, \tilde{x}; \lambda) = \underset{z}{\operatorname{argmin}} \frac{1}{2} \|z - \tilde{x}\|_2^2 + \frac{\lambda}{2} \|\text{PFS}z - d\|_2^2 \quad (6)$$

DNN architecture is an encoder-decoder U-net-type [24] convolutional network architecture with skip connections. The number of filters for both encoder and decoder layers is set to 128 and the network filter kernel size is set to 3 for both encoder and decoder layers. Mean-square-error (MSE) has been used as a Loss function and Loss minimization was performed using ADAM [15] optimizer. Since the deep network frameworks work on real-valued parameters, inputs, and outputs, in our method complex data are divided into real and imaginary parts and considered as two-channel input and output. Figure 1 illustrates the proposed ADMM based deep plug-and-play prior framework.

3. Results and Discussions

In our experiments, we have tested our method with four different datasets in order to explore the generalization potential of our method for MRI reconstruction.

First dataset has been acquired (3D MPRAGE) on six volunteers with a total of 450 brain images used as the training set. A 32-channel head coil was used for the MPRAGE

scans and the echo time (TE) of the scan was 2.17ms with a repetition time (TR) of 1.56s. We undersampled the multi-coil k-space data retrospectively with undersampling along both phase encoding dimensions (acceleration factor $R=2 \times 2$). Written, informed consent was obtained from each volunteer prior to scanning and experiments were performed in accordance with the local IRB protocol.

For the second, third, and fourth datasets, we have used three knee datasets presented by [10]. Three datasets include Coronal PD dataset (knee dataset-1), Coronal fat-saturated proton-density (PD) dataset (knee dataset-2), and Sagittal fat-saturated T2 dataset (knee dataset-3). In the knee datasets, each subjects were scanned with a 15-channel knee coil. Each of these three datasets includes a total of 200 images from 10 patients which have been used as the training set. 10 images from different patients for each dataset have used for testing purposes.

The sensitivity maps were computed from a block of size 24×24 for both brain and knee datasets using ESPIRiT [29] method. Full k-space data reconstructed with the adaptive combine method [31] was used as our gold standard for comparison. The reconstruction performance was evaluated using quantitative metrics focusing on different aspects of the reconstruction quality. The Peak Signal to Noise Ratio (PSNR) was used to assess the overall reconstructed image quality and the Structural Similarity Index (SSIM) was used to estimate the overall image similarity with respect to the reference reconstruction.

Figure 2 display the impact of acceleration factor $R=2 \times 2$ for zero-filled reconstruction, the clinical gold standard GRAPPA, and our proposed method on 3D MPRAGE brain images (brain dataset). We observed that the proposed method reconstructs artifact-free images, which is sharper and have better quality than GRAPPA reconstruction, and GRAPPA result shows noise amplification compared to our result (PSNR of ours is 52.93 compared to PSNR of 43.91 for GRAPPA). Figures 3,4 show the impact of acceleration factor $R=4$ (undersampling along only one phase encoding dimension) for zero-filled reconstruction, GRAPPA, and our proposed method on knee dataset-1 and knee dataset-2 respectively. Similar to Figure 2, GRAPPA results for knee data in Figures 3 and 4 show noise amplification compared to our results (PSNRs of ours are 41.12 and 40.48 compared to PSNRs of 30.54 and 29.39 for GRAPPA). Our results show better image restoration than GRAPPA and resulting in a nearly artifact-free reconstructed images. PSNR and SSIM quantitative variations on brain dataset is depicted in Table 1. Table 2 shows PSNR and SSIM quantitative variations on knee datasets. Tables 1,2 show that our reconstructions consistently have higher PSNRs and SSIMs than GRAPPA reconstructions.

Method	Brain Dataset	
	PSNR	SSIM
Proposed	53.3 ± 0.91	0.99 ± 0.0015
GRAPPA	44.8 ± 0.69	0.97 ± 0.0023

Table I. PSNR and SSIM variations on Brain dataset

4. Conclusion

This paper proposes an ADMM based deep plug-and-play prior framework and demonstrates the effectiveness of learning-based plug-and-play prior framework for parallel MRI reconstruction. The reported results on four real (not simulated) MRI datasets show that our proposed method outperforms the clinical gold standard GRAPPA method. We have demonstrated that the image quality arising from partially parallel MRI reconstruction can be improved, in comparison to the GRAPPA reconstruction, by using the proposed ADMM based deep plug-and-play prior framework.

Acknowledgment

This research was supported in part by NIH grants R01 NS079788, R01 EB019483, R01 DK100404, R44 MH086984, IDDC U54 HD090255, and by a research grant from the Boston Children’s Hospital Translational Research Program.

References

- [1] R. Bammer, M. Aksoy, and C. Liu. Augmented generalized sense reconstruction to correct for rigid body motion. *Magnetic Resonance in Medicine*, 57(1):90–102, 2007.
- [2] B. Bilgic, B. A. Gagoski, S. F. Cauley, A. P. Fan, J. R. Polimeni, P. E. Grant, L. L. Wald, and K. Setsompop. Wave-caipi for highly accelerated 3d imaging. *Magnetic resonance in medicine*, 73(6):2152–2162, 2015.
- [3] S. Boyd, N. Parikh, E. Chu, B. Peleato, J. Eckstein, et al. Distributed optimization and statistical learning via the alternating direction method of multipliers. *Foundations and Trends® in Machine learning*, 3(1):1–122, 2011.
- [4] F. A. Breuer, M. Blaimer, M. F. Mueller, N. Seiberlich, R. M. Heidemann, M. A. Griswold, and P. M. Jakob. Controlled aliasing in volumetric parallel imaging (2d caipirinha). *Magnetic resonance in medicine*, 55(3):549–556, 2006.
- [5] S. H. Chan, X. Wang, and O. A. Elgandy. Plug-and-play admm for image restoration: Fixed-point convergence and applications. *IEEE Transactions on Computational Imaging*, 3(1):84–98, 2017.
- [6] M. A. Griswold, P. M. Jakob, R. M. Heidemann, M. Nittka, V. Jellus, J. Wang, B. Kiefer, and A. Haase. Generalized autocalibrating partially parallel acquisitions (grappa). *Magnetic resonance in medicine*, 47(6):1202–1210, 2002.
- [7] M. A. Griswold, P. M. Jakob, M. Nittka, J. W. Goldfarb, and A. Haase. Partially parallel imaging with localized sensitivities (pils). *Magnetic Resonance in Medicine*, 44(4):602–609, 2000.
- [8] M. Guerquin-Kern, L. Lejeune, K. P. Pruessmann, and M. Unser. Realistic analytical phantoms for parallel magnetic resonance imaging. *IEEE Transactions on Medical Imaging*, 31(3):626–636, 2012.
- [9] J. P. Haldar. Low-rank modeling of local k -space neighborhoods (loraks) for constrained mri. *IEEE transactions on medical imaging*, 33(3):668–681, 2014.
- [10] K. Hammernik, T. Klatzer, E. Kobler, M. P. Recht, D. K. Sodickson, T. Pock, and F. Knoll. Learning a variational network for reconstruction of accelerated mri data. *Magnetic resonance in medicine*, 79(6):3055–3071, 2018.
- [11] K. Heberlein and X. Hu. Auto-calibrated parallel spiral imaging. *Magnetic resonance in medicine*, 55(3):619–625, 2006.
- [12] R. M. Heidemann, M. A. Griswold, A. Haase, and P. M. Jakob. Vd-auto-smash imaging. *Magnetic resonance in medicine*, 45(6):1066–1074, 2001.
- [13] P. M. Jakob, M. A. Griswold, R. R. Edelman, and D. K. Sodickson. Auto-smash: a self-calibrating technique for smash imaging. *Magnetic Resonance Materials in Physics, Biology and Medicine*, 7(1):42–54, 1998.
- [14] U. S. Kamilov, H. Mansour, and B. Wohlberg. A plug-and-play priors approach for solving nonlinear imaging inverse problems. *IEEE Signal Processing Letters*, 24(12):1872–1876, 2017.
- [15] D. P. Kingma and J. Ba. Adam: A method for stochastic optimization. *arXiv preprint arXiv:1412.6980*, 2014.
- [16] W. E. Kyriakos, L. P. Panych, D. F. Kacher, C.-F. Westin, S. M. Bao, R. V. Mulkern, and F. A. Jolesz. Sensitivity profiles from an array of coils for encoding and reconstruction in parallel (space rip). *Magnetic Resonance in Medicine*, 44(2):301–308, 2000.
- [17] D. Liang, B. Liu, J. Wang, and L. Ying. Accelerating sense using compressed sensing. *Magnetic Resonance in Medicine*, 62(6):1574–1584, 2009.
- [18] C. Liu, R. Bammer, and M. E. Moseley. Parallel imaging reconstruction for arbitrary trajectories using k -space sparse matrices (kspace). *Magnetic resonance in medicine*, 58(6):1171–1181, 2007.
- [19] M. Lustig, D. Donoho, and J. M. Pauly. Sparse mri: The application of compressed sensing for rapid mr imaging. *Magnetic resonance in medicine*, 58(6):1182–1195, 2007.
- [20] M. Lustig and J. M. Pauly. Spirit: Iterative self-consistent parallel imaging reconstruction from arbitrary k -space. *Magnetic resonance in medicine*, 64(2):457–471, 2010.
- [21] K. P. Pruessmann, M. Weiger, P. Börner, and P. Boesiger. Advances in sensitivity encoding with arbitrary k -space trajectories. *Magnetic resonance in medicine*, 46(4):638–651, 2001.
- [22] K. P. Pruessmann, M. Weiger, M. B. Scheidegger, P. Boesiger, et al. Sense: sensitivity encoding for fast mri. *Magnetic resonance in medicine*, 42(5):952–962, 1999.
- [23] S. Ramani and J. A. Fessler. Parallel mr image reconstruction using augmented lagrangian methods. *IEEE Transactions on Medical Imaging*, 30(3):694–706, 2011.
- [24] O. Ronneberger, P. Fischer, and T. Brox. U-net: Convolutional networks for biomedical image segmentation. In

Method	Knee Dataset-1		Knee Dataset-2		Knee Dataset-3	
	PSNR	SSIM	PSNR	SSIM	PSNR	SSIM
Proposed	42.28 ± 1.31	0.96 ± 0.0108	39.87 ± 1.08	0.93 ± 0.0086	44.09 ± 2.85	0.95 ± 0.053
GRAPPA	30.27 ± 0.89	0.71 ± 0.081	28.43 ± 0.97	0.6 ± 0.045	31.91 ± 1.54	0.7 ± 0.063

Table 2. PSNR and SSIM variations on Knee datasets-1,2,3

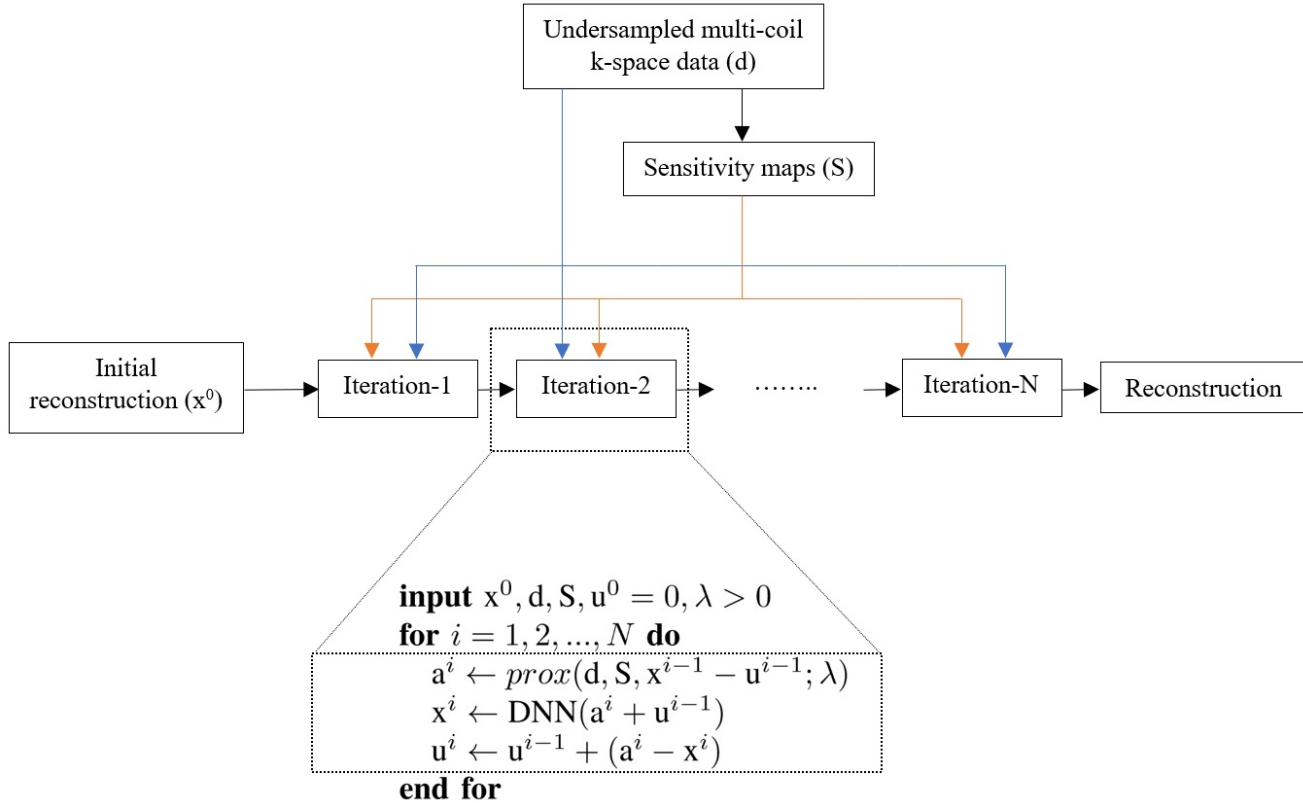


Figure 1. Proposed deep plug-and-play prior framework.

International Conference on Medical image computing and computer-assisted intervention, pages 234–241. Springer, 2015.

- [25] N. Seiberlich, F. Breuer, R. Heidemann, M. Blaimer, M. Griswold, and P. Jakob. Reconstruction of undersampled non-cartesian data sets using pseudo-cartesian grappa in conjunction with grog. *Magnetic resonance in medicine*, 59(5):1127–1137, 2008.
- [26] D. K. Sodickson and W. J. Manning. Simultaneous acquisition of spatial harmonics (smash): fast imaging with radiofrequency coil arrays. *Magnetic resonance in medicine*, 38(4):591–603, 1997.
- [27] S. Sreehari, S. V. Venkatakrishnan, B. Wohlberg, G. T. Buzzard, L. F. Drummy, J. P. Simmons, and C. A. Bouman. Plug-and-play priors for bright field electron tomography and sparse interpolation. *IEEE Transactions on Computational Imaging*, 2(4):408–423, 2016.
- [28] Y. Sun, B. Wohlberg, and U. S. Kamilov. An online plug-

and-play algorithm for regularized image reconstruction. *IEEE Transactions on Computational Imaging*, 2019.

- [29] M. Uecker, P. Lai, M. J. Murphy, P. Virtue, M. Elad, J. M. Pauly, S. S. Vasanawala, and M. Lustig. Espiritan eigenvalue approach to autocalibrating parallel mri: where sense meets grappa. *Magnetic resonance in medicine*, 71(3):990–1001, 2014.
- [30] S. V. Venkatakrishnan, C. A. Bouman, and B. Wohlberg. Plug-and-play priors for model based reconstruction. In *2013 IEEE Global Conference on Signal and Information Processing*, pages 945–948. IEEE, 2013.
- [31] D. O. Walsh, A. F. Gmitro, and M. W. Marcellin. Adaptive reconstruction of phased array mr imagery. *Magnetic Resonance in Medicine*, 43(5):682–690, 2000.
- [32] A. P. Yazdanpanah and E. E. Regentova. Compressed sensing magnetic resonance imaging based on shearlet sparsity and nonlocal total variation. *Journal of Medical Imaging*, 4(2):026003, 2017.

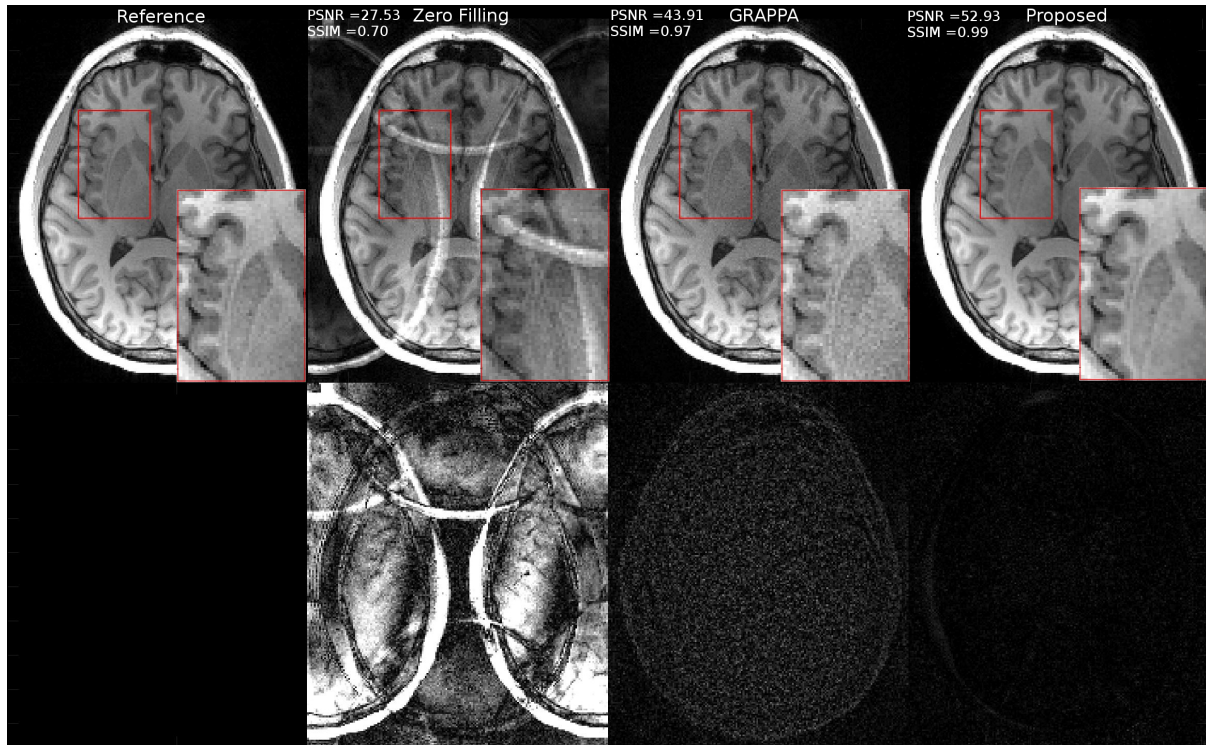


Figure 2. First row (left to right): Gold standard reconstruction result using fully sampled data, zero-filled reconstruction, GRAPPA reconstruction result with undersampling factor of 2×2 , and our reconstruction result with undersampling factor of 2×2 for 3D MPRAGE data. Second row, includes error maps correspond to each reconstruction results for comparison.

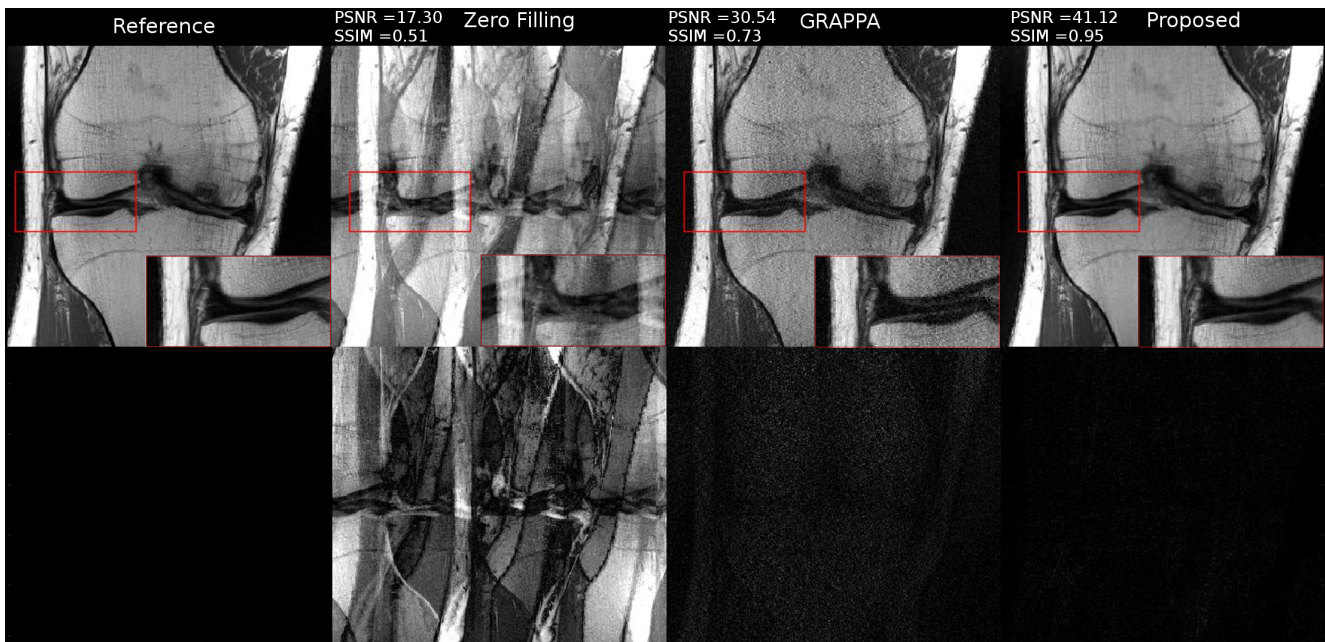


Figure 3. First row (left to right): Gold standard reconstruction result using fully sampled data, zero-filled reconstruction, GRAPPA reconstruction result with undersampling factor of 4, and our reconstruction result with undersampling factor of 4 for 2D Coronal PD data. Second row, includes error maps correspond to each reconstruction results for comparison.

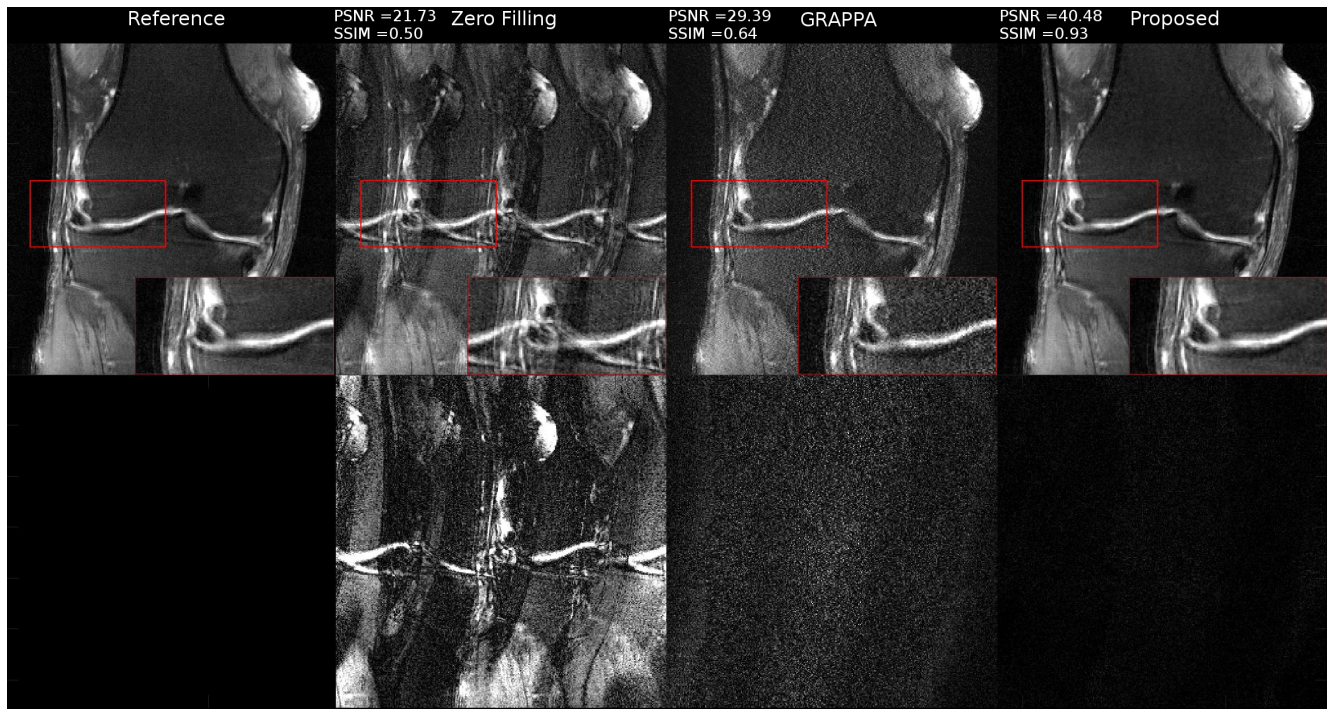


Figure 4. First row (left to right): Gold standard reconstruction result using fully sampled data, zero-filled reconstruction, GRAPPA reconstruction result with undersampling factor of 4, and our reconstruction result with undersampling factor of 4 for 2D Coronal fat-saturated PD data. Second row, includes error maps correspond to each reconstruction results for comparison.

- [33] A. P. Yazdanpanah and E. E. Regentova. Compressed sensing mri using curvelet sparsity and nonlocal total variation: Cs-nltv. *Electronic Imaging*, 2017(13):5–9, 2017.
- [34] E. N. Yeh, C. A. McKenzie, M. A. Ohliger, and D. K. Sodickson. 3parallel magnetic resonance imaging with adaptive radius in k-space (pars): Constrained image reconstruction using k-space locality in radiofrequency coil encoded data. *Magnetic resonance in medicine*, 53(6):1383–1392, 2005.